International Journal of
Environmental Research and Public Health

MDPI

Article

Effects of Tidal Scenarios on the Methane Emission Dynamics in the Subtropical Tidal Marshes of the Min River Estuary in Southeast China

Jiafang Huang [1], Min Luo [2,*], Yuxiu Liu [1,3], Yuxue Zhang [1,3] and Ji Tan [1,3]

1 Institute of Geography, Fujian Normal University, Fuzhou 350007, China
2 Environment and Resource College, Fuzhou University, Fuzhou 350116, China
3 School of Geographical Sciences, Fujian Normal University, Fuzhou 35007, China
* Correspondence: luomin@fzu.edu.cn; Tel.: +86-0591-2286-6070; Fax: +86-0591-2286-6070

Received: 21 June 2019; Accepted: 2 August 2019; Published: 5 August 2019

Abstract: In order to accurately estimate the effects of tidal scenarios on the CH_4 emission from tidal wetlands, we examined the CH_4 effluxes, dissolved CH_4 concentrations, and environmental factors (including in situ pH, Eh and electrical conductivity, porewater SO_4^{2-}, NO_3^-, and NH_4^+) during inundation and air-exposure periods in high- and low-tide seasons in the Min River Estuary in southeast China. By applying static and floating chambers, our results showed that the CH_4 effluxes during the inundation periods were relatively constant and generally lower than those during the air-exposed periods in both seasons. When compared, the CH_4 effluxes during the air-exposed periods were significantly higher in the high-tide season than those in the low-tide season. In contrast, CH_4 effluxes during the inundation periods were significantly lower in the high-tide season than those in the low-tide season. During the inundation periods, dissolved CH_4 concentrations were inversely proportional to in situ Eh. Under air-exposed conditions, CH_4 effluxes were proportional to in situ pH in both seasons, while the dissolved CH_4 concentrations were negatively correlated with the porewater SO_4^{2-} concentrations in both seasons. Our results highlighted that CH_4 effluxes were more dynamic between inundation and air-exposure periods compared to low- and high-tide seasons.

Keywords: tide; inundation; methane efflux; dissolved methane; tidal wetland; Min River Estuary

1. Introduction

Methane (CH_4) is the second-most important radiatively active greenhouse gas and has a global warming potential 28 times greater than that of carbon dioxide (CO_2) over a 100-year time span [1]. Despite a relatively small surface area, the volume of coastal CH_4 effluxes was estimated to be quantitatively comparable to the CH_4 uptake by the continental shelf [2]. Tidal wetlands, with an average net primary productivity of 930–7600 g C $m^{-2}{\cdot}yr^{-1}$ [3], are important contributors of coastal CH_4 effluxes [4]. Even though the quantification of CH_4 effluxes from estuarine tidal wetlands is crucial when evaluating the global greenhouse budget, the data available for this purpose is extremely limited as estuarine tidal wetlands are periodically affected by fluctuating tidal hydrologic regimes [5].

The action of tides has a significant effect on CH_4 effluxes through various physical, geochemical, and biological factors. First, tidal activity can induce changes in the hydrodynamic conditions, sediment deposition, and transport, as well as in the influxes and effluxes of mineral and organic compounds [6–8]. Second, tidal water is rich in oxygen (O_2), sulfate (SO_4^{2-}), and high in salinity, which significantly affects methanogenesis and CH_4 oxidation [9,10]. Third, the tides also influence various biological processes that have the potential to modify carbon cycling, such as microbial and plant respiration, photosynthesis, and carbon uptake [11,12].

Temporal variations in tidal activity can result in CH_4 efflux dynamics [13]. Generally, studies on the impact of tidal activity on CH_4 effluxes in estuarine tidal wetlands are based on a tidal, diel, or seasonal sampling timescale [5,14–16]. For instance, Hirota et al. [17] examined CH_4 effluxes at 6 h intervals from 19 to 22 August along the sandy shore of Japan in mid-summer 2003; Rosentreter et al. [18] studied CH_4 effluxes over 24-h periods in the wet and dry seasons in mangrove creeks along the north-eastern coast of Queensland, Australia, between March 2016 and March 2018; and Jacotot et al. [5] monitored CH_4 emissions every three weeks throughout the high-tide period from the beginning of flooding to the end of the ebb in a Rhizophora mangrove forest (New Caledonia) from December 2016 to September 2017. In other research, Li et al. [19] continuously measured CH_4 effluxes for two years using the eddy covariance technique in a subtropical salt marsh in eastern China in 2011 and 2012. A notable finding in previous studies was that CH_4 effluxes exhibit a significant seasonal pattern with respect to tidal activity.

The coastal zone of China includes an 1800 km coastline that stretches across tropical, subtropical, and temperate zones and an extensive tidal wetland with an area of approximately 5.8×10^4 km^2 [20]. The tidal marshes of the Min River Estuary in the East China Sea cover ca. 21 km^2 of subtropical coastal wetland. In the Min River Estuary, strong astronomical tides always occur between September and October. This is the combined result of the thermal expansion of seawater, the autumnal equinoctial spring tide, the western propagation of typhoons across the Pacific Ocean, and a reduction in river runoff [21]. During this period, the tide heights are significantly higher, the inundation periods are prolonged compared to other seasons, and the entire tidal flat is flooded most of the time. In contrast, during the winter and early spring, the tide height is much lower, the inundation period is significantly shorter, and the tide at times does not even reach the middle or upper regions of the tidal flats [22]. Previous studies have suggested that seasonal dynamics were apparent in the CH_4 effluxes in the tidal wetlands of the Min River Estuary in the East China Sea, and that the highest CH_4 effluxes occurred during the summer months (June to August) [22–25]. However, none of these investigated the influence of tidal activities on the dynamics of CH_4 effluxes.

To explore this issue, in this study, the CH_4 effluxes, dissolved CH_4 concentrations, and environmental factors (including in situ pH, Eh and electrical conductivity (EC), porewater SO_4^{2-}, NO_3^-, and NH_4^+) were investigated in the tidal marshes of the Min River Estuary on an hourly basis from 26 September to 2 October 2011, and 23 March to 27 March 2012. The specific aims were (i) to explore the changes in the CH_4 effluxes over seasonal and tidal scales, and (ii) to identify the environmental factors driving the dynamics of CH_4 effluxes during the inundated and air-exposed periods.

2. Materials and Methods

2.1. Site and Sampling Period Description

Located in the transitional zone between the middle and south subtropical zones, the Min River flows past vast tidal wetlands along the margins of its estuary in the East China Sea (Figure 1a,b). The tide of the Min River Estuary is a regular semi-diurnal tide with a range of 2.5–6.0 m, based on the data from the hydrological station (26°06′49″ N, 119°40′19″ E) of the China National Oceanic Bureau (http://ocean.cnss.com.cn/). The selected sampling site is located in a middle littoral zone within the Shanyutan brackish tidal marsh (26°1′–26°3′ N, 119°36′–119°38′ E). The site is primarily covered by the dominant species *Cyperus malaccensis* (also known as saltwater grass), a plant species of thin long sedge. The sediment is characterized by silty loam texture (i.e., 16–30% clay, 57–70% silt, and 7–12% sand).

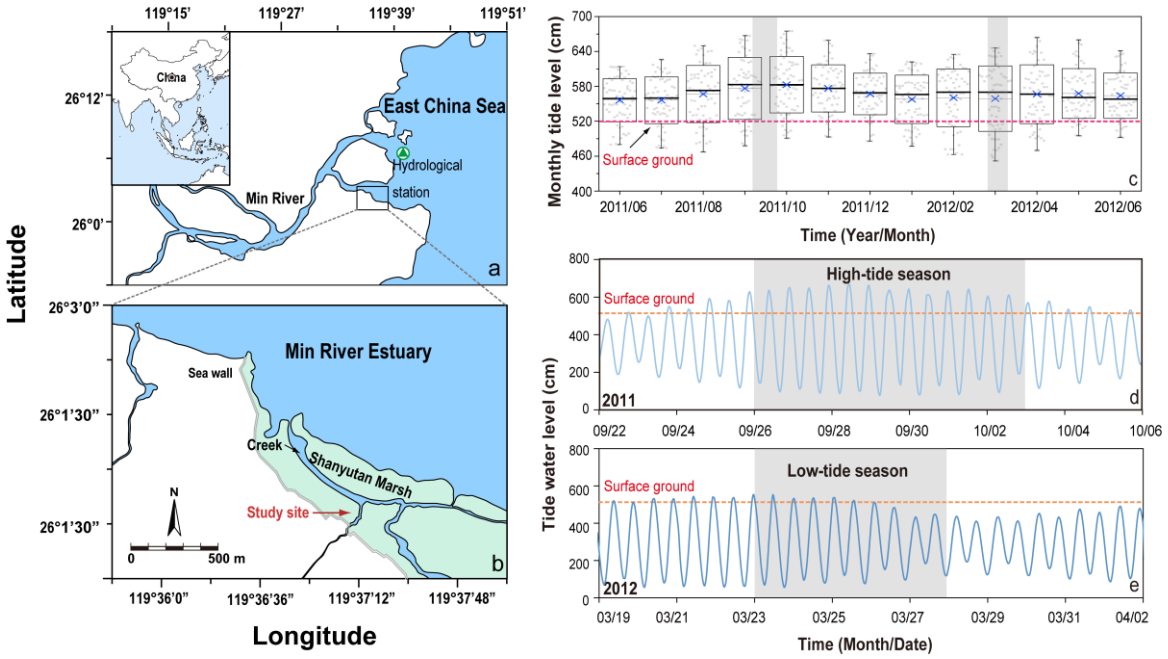

Figure 1. (**a**) Location of the study site in the Shanyutan brackish tidal marsh of the East China Sea, (**b**) the Min River Estuary, (**c**) patterns of tidewater level fluctuation (in cm) as assessed by the nearby hydrological station: monthly variation in the tide water level from June 2011 to June 2012, (**d**) daily tidewater level from 22 September to 6 October 2011, and (**e**) from 19 March to 2 April 2012. The shadow denotes the sampling period for the CH_4 and porewater inventories. The red line denotes the surface of the ground at the study site. The tidewater level data was collected from the Chuanshi bathymetric benchmark (26°06′49″ N, 119°40′19″ E) of the China National Oceanic Bureau.

2.2. Sample Collection and Handling

In this study, we defined the study period from 26 September to 2 October 2011 as the 'high-tide season', and that from 23 March to 27 March 2012 as the 'low-tide season'. The sampling was conducted from 7:00 to 17:00 during the high-tide season and from 8:00 to 18:00 during the low-tide season. Enclosed static chambers were used to measure CH_4 effluxes at the sediment–air interface during the air-exposed periods (Figure 2a), while floating chambers were used to measure the CH_4 effluxes at the water–air interface during the inundation periods (Figure 2b). The enclosed static chamber was composed of two parts: a polyvinyl chloride bottom collar (diameter: 30 cm; depth: 25 cm), and a chamber body (diameter: 30 cm; height: 120 cm) with a temperature-humidity-pressure sensor and a small fan. The bottom collar was inserted into the wetland sediments, protruding 20 cm out of the sediment surface, approximately 7 d prior to the first sampling. The floating chambers (diameter: 30 cm; height: 40 cm) were made of transparent plexiglass; they were also provided with a temperature-humidity-pressure sensor and a small fan. Instead of a bottom collar, the floating chambers were set on swimming rings made of thick rubber. To prevent movement of the floating chambers during tidal fluctuation, the chambers were fixed by pipes inserted into the ground; therefore, the floating chambers could move up and down depending on the changes in tidewater height [22]. Triplicate enclosed static or floating chambers were separated from each other by approximately 10 m. Efflux measurements were conducted every 60 min during the air-exposed periods and every 45 min during the inundation periods. After the settling of the chamber bodies, all the edges were sealed with silicon and adhesive tape to ensure enough airtightness. Next, the fans were turned on and 30 mL of gas was immediately extracted with a syringe, and the operation was repeated thrice at 15 min intervals during each sampling period. Once a sampling cycle was completed, the chambers were removed and vented before the next sampling. Gas samples were collected in a vacuum-sealed 50 mL aluminum foil sampling bag (Delin Ltd., DaLian, China).

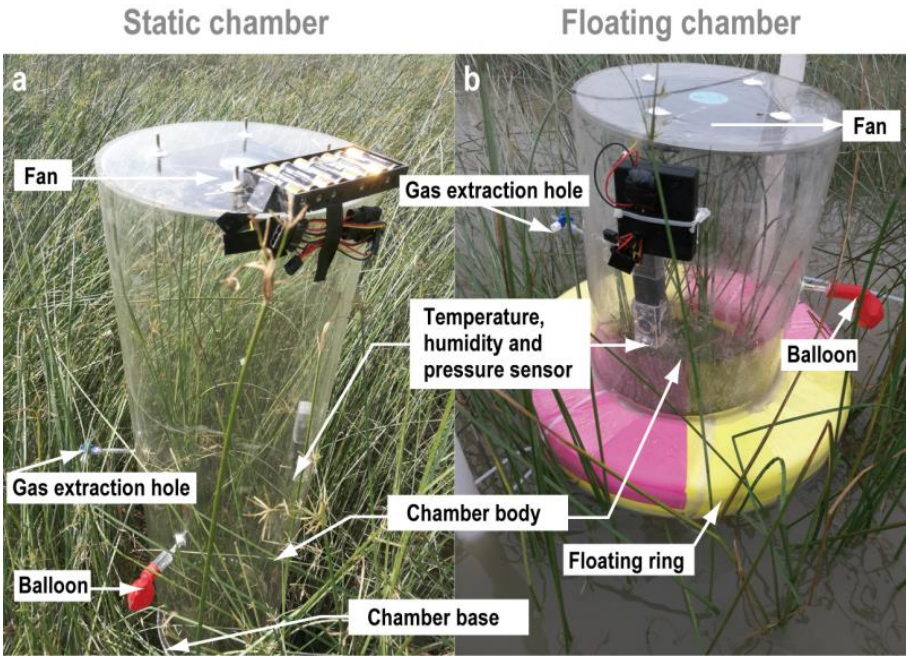

Figure 2. (**a**) Enclosed static chambers were used to measure the CH_4 effluxes in the wetland at the sediment–air interface during the air-exposure period, and (**b**) floating chambers were used to measure the CH_4 effluxes at the water–air interface during the tidal inundation period.

At each study location, triplicate rhizon samplers (20 mL) were installed on the sediment surface (10–15 cm) to collect porewater over time. Porewater was collected using in-situ rhizon samplers composed of a 0.15 µm hydrophilic porous polymer. All the gas and porewater were placed into sealed bags, and porewater subsamples were transported to the laboratory in an icebox (~4 °C).

2.3. Gas Flux Analysis and Estimation

Methane concentrations were determined using a gas chromatograph (GC-2014, Shimadzu, Kyoto, Japan) equipped with a thermal conductivity detector and a pulsed discharge detector. The column and detector temperatures were set at 60 °C. The carrier gas was high-purity helium, with a flow rate of 30 mL·min^{-1}. Standard CH_4 gas was produced by the Chinese Academy of Metrology (http://www.nim.ac.cn). The formula for calculating the gas flux is shown in Equation (1) [26,27]:

$$F = \frac{1000}{V} \cdot \frac{dc}{dt} \cdot H \cdot \left(\frac{273}{273 + T}\right), \quad (1)$$

where F is the CH_4 efflux (µmol·m^{-2}·h^{-1}), V is the molar volume of gas (22.4 L·mol^{-1}) under standard atmospheric pressure, dc/dt is the CH_4 gas concentration per unit time change (µL·L^{-1}·h^{-1}) in the static chamber, H is the chamber height (m), and T is the sampling temperature.

2.4. Environmental Traits

Tide height (based on the ground surface) was recorded using a stainless steel water-level gauge every 15 min during the inundation periods. Tidewater salinity was examined by a SALT6+ salinity meter (EUTECH Instruments, Vernon Hills, IL, USA). Air temperature, precipitation, and humidity data were recovered from the U30-NRC HOBO weather station (Onset Computer Corporation, Bourne, MA, USA). In situ temperatures were measured using an IQ150 instrument (IQ Scientific Instruments, Carlsbad, CA, USA). The five-year tide water height and tide inundation frequency were obtained from Solinst 3001 (Solinst Canada Ltd., Georgetown, ON, Canada) data-loggers (±0.01 m) at 30-min intervals and were corrected by the China National Oceanic Bureau.

2.5. Sediment and Porewater Geochemistry

In situ electrical conductivity (EC) was measured with a Fieldscout 2265FS EC meter (Spectrum Technologies, Dallas, TX, USA). The in situ pH and Eh values were determined using an Orion 3-Star Plus pH/Eh benchtop meter (Thermo Fisher Scientific Inc., Waltham, MA, USA). In the laboratory, all porewater samples were handled under a nitrogen atmosphere. The porewater was filtered with 0.22 μm filters into 10 mL glass vials that were then capped with butyl rubber septa. The porewater subsamples were preserved at 4 °C and were analyzed within a month. Porewater SO_4^{2-} concentrations were determined using ICS-2000 ion chromatography (Dionex, Sunnyvale, CA, USA). Porewater NO_3^- and NH_4^+ concentrations were determined using a SAN++ flow injection system (Skalar Co., Breda, The Netherlands). The detection limits were 1 μM/8% for SO_4^{2-}, 10 μM/6% for NO_3^-, and 1 μM/4% for NH_4^+.

The dissolved CH_4 concentration was determined using a headspace equilibration technique developed by Keller et al. [28] and Tong et al. [26]. Briefly, 15 mL of the first syringe porewater sample, obtained using rhizon samplers, was filtered through N_2 preleached syringe filters (0.45 μm-pore) into a pre-vacuum glass scintillation vial, and was supplemented with 15 mL N_2 to balance the difference in air pressure inside and outside the vial. For sterilization, 0.1 mL of saturated $HgCl_2$ solution was injected into the vials. The bottles were then vigorously shaken for 30 s and placed on a rotary shaker (240 rpm, ambient temperature) for 0.5 h to ensure that all dissolved CH_4 had escaped into the bottle headspace. The CH_4 concentrations were measured using a GC2014 gas chromatograph with a flame-ionization detector (Shimadzu, Kyoto, Japan), typically within 2 h of collection. The measured CH_4 concentrations were corrected for standard pressure and temperature using the ideal gas law and were multiplied by the headspace volume [26].

2.6. Data Analysis

All datasets were tested before the analysis of variance (ANOVA) to check that they meet the assumptions of homogeneity (the Brown and Forsythe test) and normality (the Shapiro–Wilk test). In cases where the data did not satisfy this assumption, the raw data were subjected to a log-transformation before further statistical analysis. A two-way analysis of variance (ANOVA) was used to determine whether the tide inundation periods (i.e., inundation and air-exposed periods), seasonality (i.e., low- and high-tide seasons), or an interaction between the two affected the soil CH_4 effluxes or dissolved CH_4 concentrations, as well as the environmental factors (in situ pH, Eh, and EC; porewater SO_4^{2-}, NO_3^-, and NH_4^+). The ANOVA tests were followed with an independent *t*-test to determine the difference between low- and high-tide seasons within each period, or between inundation and air-exposed periods within each season. Finally, nonlinear regressions between tide height and CH4 effluxes, between dissolved CH_4 concentrations and in situ Eh during the inundation periods; linear regressions were used between the CH_4 effluxes (or dissolved CH_4 concentrations) and other environmental parameters during the air-exposed periods. All of the data in this study is presented in the form of the mean ± standard error (SE), unless otherwise indicated. All of the statistical analyses in this study were conducted using the SPSS Statistics 22.0 software program with a significance level of 0.05.

3. Results

Between June 2011 and June 2012, the monthly tide heights were the lowest in March and the highest between September and October (Figure 1c). Other hydrological and climatic condition data obtained during the two study periods are listed in Table 1. The mean inundation duration per day ranged from 2.2 h in the low-tide season to 8.1 h in the high-tide season (Table 1) and the monthly tide heights (with respect to the surface of the ground) were 123.7 cm and 16.4 cm in the high- and low-tide seasons, respectively (Table 1). The air temperature in the high-tide season (22.1 ± 0.1 °C) was relatively high compared with that in the low-tide season (17.5 ± 0.1 °C), and the humidity levels were

comparable in the two seasons (Table 1). During the high-tide season, the salinity of the tide water was approximately 3.32 ppt, while during the low-tide season, the salinity of the tide water dropped to 0.73 ppt, possibly due to a heavy spring rainfall that diluted the salts and nutrients in the river or sea water.

Table 1. Hydrological and climatic conditions (mean ± SE) of high- and low-tide seasons in the tidal wetlands of the Min River Estuary, East China Sea.

	High-Tide Season	Low-Tide Season
Sampling period	26 September to 2 October 2011	23 to 27 March 2012
Mean air temperature (°C)	22.1 ± 0.1	17.5 ± 0.1
Mean humidity (%)	90.5 ± 0.3	99.9 ± 0.1
Mean highest tidal height (cm) *	123.7 ± 7.4	16.4 ± 11.1
Mean inundation duration per day (h)	8.1 ± 5.1	2.2 ± 1.4
Mean tidewater salinity (ppt)	3.32 ± 0.15	0.73 ± 0.01

Note: * Tidal height was calculated based on the surface ground of study site.

3.1. Temporary Dynamics in CH_4 Effluxes, Dissolved CH_4 Concentrations, and Porewater Geochemistries

During the high-tide season, the sediments were inundated every day (Figure 3a). The tidal inundation periods first increased from 3.3 h to 4 h and then declined to 2.9 h, and were accompanied by a gradual increase in the maximal tide height from 113 cm to 140 cm, followed by a decline to 106 cm (Figure 3a). During the low-tide season, the tidal inundation periods gradually decreased from 1.9 h to 0.6 h, and the maximal inundation height gradually decreased from 44 cm to 8 cm (Figure 4a). The tide did not reach the study site in the last two days of the low-tide season (Figure 4a).

The CH_4 effluxes (given in $\mu mol \cdot m^{-2} \cdot h^{-1}$, Figures 3a and 4a) ranged from 1.0 to 248.3. During both the high- and low-tide seasons, the CH_4 effluxes during the inundation periods were much lower than those during the air-exposed periods (Figure 5a) and the dissolved CH_4 concentrations (given in μM, Figures 3d and 4d) generally followed a trend similar to that of the CH_4 effluxes ($r = 0.47$, $p < 0.001$, $n = 258$), i.e., they were low during the inundation periods (<5 μM) and much higher during the air-exposed periods (8.3 to 103.29 μM) in both seasons (Figures 3d and 4d). Regarding the differences between the two seasons, the CH_4 effluxes and dissolved CH_4 concentrations from air-exposed sediments were significantly higher during the high-tide season compared with the low-tide season, while the CH_4 effluxes and concentrations of dissolved CH_4 during the inundation periods were significantly lower during the high-tide season compared with the low-tide season (Figure 5a,b).

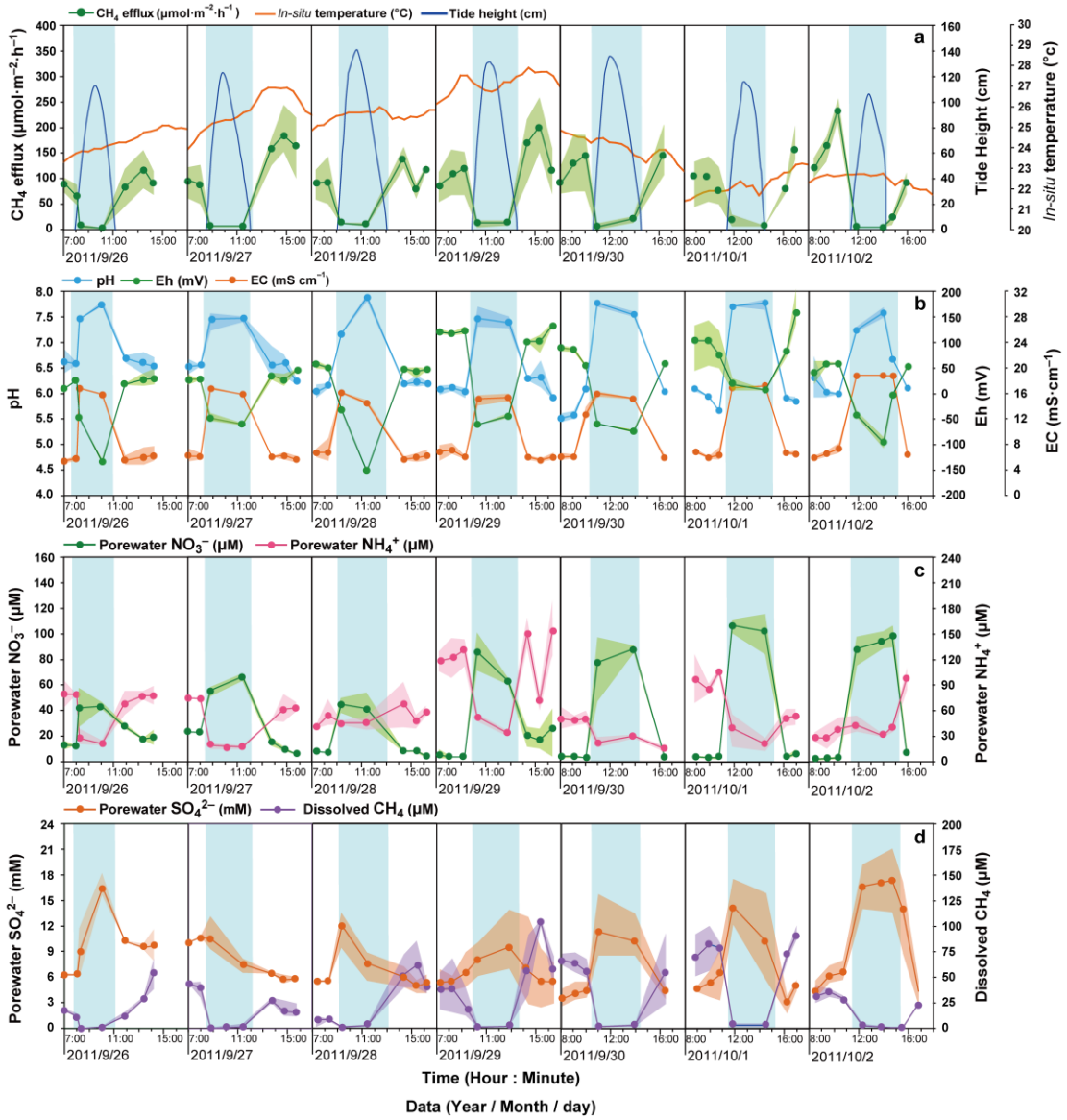

Figure 3. Dynamics of (**a**) the tide height (cm, water level above the ground surface), in situ temperature (°C), and CH_4 effluxes (μmol·m^{-2}·h^{-1}); (**b**) EC (mS·cm^{-1}), porewater pH, and Eh (mV); (**c**) NO_3^- (μM) and NH_4^+ (μM); (**d**) SO_4^{2-} (mM) and dissolved CH_4 (μM) from tidal cycles in the period from 26 September 2011 to 2 October 2011 in the tidal wetlands of the Min River Estuary. The blue belt denotes the tidal inundation period and the shaded areas around the data denote the standard error.

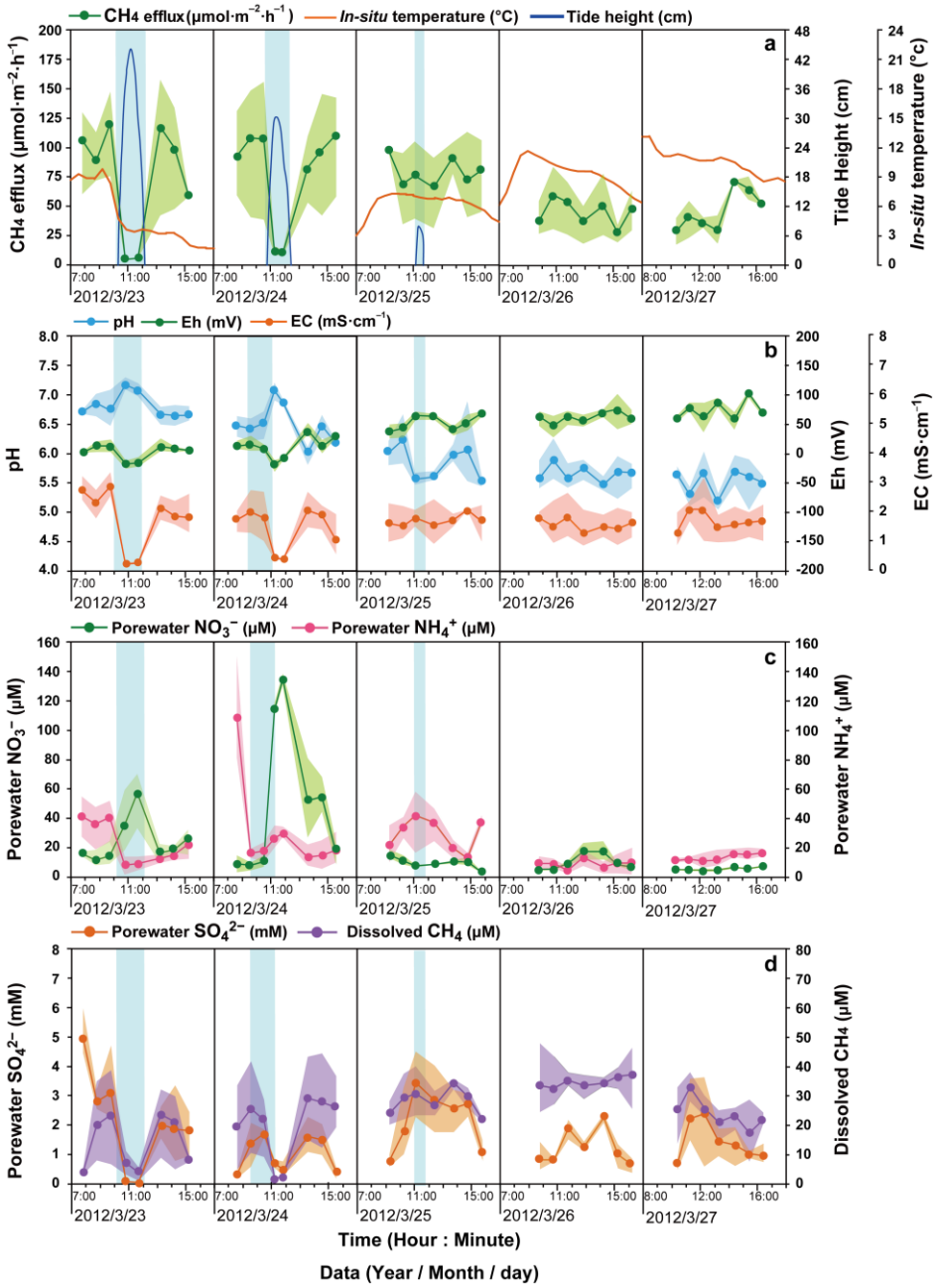

Figure 4. Dynamics of the (**a**) tide height (cm, water level above the ground surface), in situ temperature (°C), and CH_4 effluxes (μmol·m^{-2}·h^{-1}); (**b**) EC (mS·cm^{-1}), porewater pH, and Eh (mV); (**c**) NO_3^- (μM) and NH_4^+ (μM); (**d**) SO_4^{2-} (mM) and dissolved CH_4 (μM) during tidal cycles between 23 March 2012 and 27 March 2012 in the sediments of the tidal wetland of the Min River Estuary. The blue belt denotes the tidal inundation period. The shaded areas around the data denote the standard error.

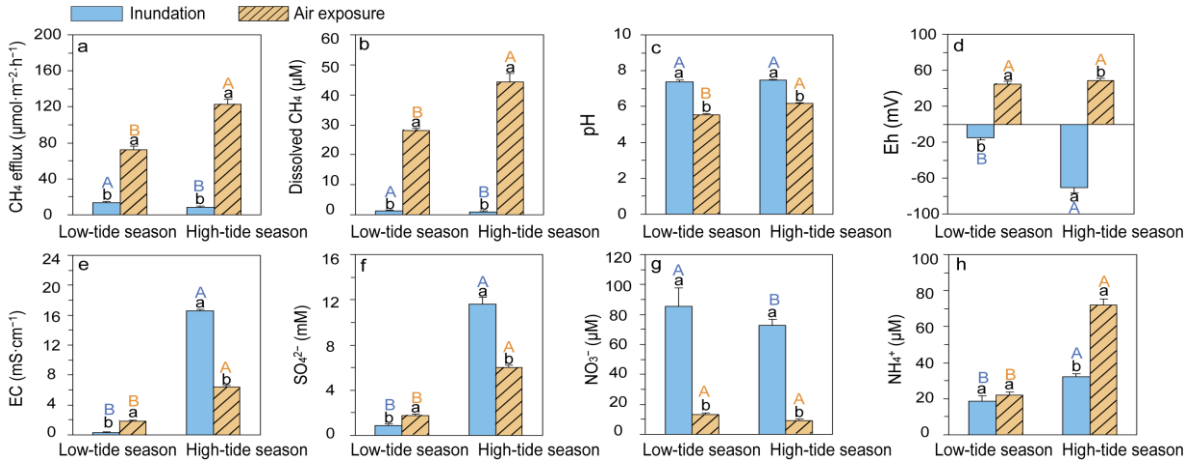

Figure 5. (**a**) CH_4 effluxes (μmol·m^{-2}·h^{-1}), (**b**) dissolved CH_4 (μM), (**c**) in situ pH, (**d**) Eh (mV), (**e**) EC (mS·cm^{-1}), (**f**) porewater SO_4^{2-} (mM), (**g**) porewater NO_3^- (μM), and (**h**) NH_4^+ (μM) in the tidal wetlands of the Min River Estuary. The solid blue and shadowed orange bars denote inventories made during inundation and air exposure periods, respectively. The capital letters in colors indicate significant differences ($p < 0.05$ after an independent *t*-test) between the low- and high-tide seasons. The small letters in black indicate significant differences ($p < 0.05$ after the independent *t*-test) between the inundation and air-exposed periods.

3.2. Difference in CH_4 Effluxes, Dissolved CH_4 Concentrations, and Porewater Geochemistries

The results of a two-way ANOVA showed that both the tide inundation and seasonality affected the CH_4 effluxes, dissolved CH_4 concentrations, in situ pH, Eh and EC, concentrations of porewater SO_4^{2-}, NO_3^-, and NH_4^+ (Table 2).

Table 2. Summary of a two-way ANOVA on the effects of tide inundation, seasonality, and their interaction on the methane effluxes and dissolved CH_4; the in situ pH, Eh, and EC; and the porewater SO_4^{2-}, NO_3^-, and NH_4^+ in the tidal marsh of the Min River Estuary, East China Sea.

Source	Tide Inundation		Season		Inundation × Season	
	F Value	*p* Value	*F* Value	*p* Value	*F* Value	*p* Value
CH_4 efflux	140.173	<0.001	12.842	<0.001	10.340	0.001
Dissolved CH_4	116.379	<0.001	6.695	0.010	6.291	0.013
In situ pH	275.113	<0.001	19.358	<0.001	3.151	0.077
In situ Eh	361.573	<0.001	29.322	<0.001	39.922	<0.001
In situ EC	502.431	<0.001	2932.265	<0.001	903.409	<0.001
Porewater SO_4^{2-}	31.943	<0.001	321.832	<0.001	60.722	<0.001
Porewater NO_3^-	525.225	<0.001	7.388	0.007	2.169	0.142
Porewater NH_4^+	21.983	<0.001	47.971	<0.001	15.693	<0.001

The in situ pH was slightly acidic during the air-exposed periods (low-tide season: 5.55; high-tide season: 6.28) and turned neutral (low-tide season: 7.05; high-tide season: 7.39) during the inundation periods in both seasons (Figure 5c). Moreover, in situ Eh was negative during the inundation periods (low-tide season: −15.26; high-tide season: −70.62) and became positive (low-tide season: 48.91; high-tide season: 54.82) during the air-exposed periods in both seasons (Figure 5d).

During the low-tide season, the in situ EC (mS·cm^{-1}; Figure 5e) and SO_4^{2-} concentrations (mM; Figure 5f) were much lower during the inundation periods (EC = 0.34; SO_4^{2-} = 0.86) than during the air-exposed periods (EC = 1.77; SO_4^{2-} = 1.77). In contrast, during the high-tide season, the in situ EC and porewater SO_4^{2-} were much higher during the inundation periods (EC = 16.53; SO_4^{2-} = 11.63) than during the air-exposed periods (EC = 6.43; SO_4^{2-} = 6.01).

During inundation, porewater NO_3^- (low-tide season = 85.24; high-tide season = 72.84) was much higher than that during the air-exposed periods (low-tide season = 13.06; high-tide season = 9.38) in both seasons (Figure 5g). In addition, both inundated and air-exposed porewater NH_4^+ were relatively less abundant in the low-tide season (inundation = 17.75; air-exposed = 20.65) compared with the high-tide season (inundation = 32.19; air-exposed = 72.15; Figure 5h).

3.3. Relation between CH_4 Effluxes or Dissolved CH_4 Concentrations and Other Environmental Factors

During the inundation periods, CH_4 effluxes and dissolved CH_4 concentrations exponentially declined with an increase in tide heights and Eh, respectively (Figure 6a,b). During the air-exposed periods, CH_4 effluxes linearly increased with a promotion in in situ pH (Figure 6c), and dissolved CH_4 concentrations declined with an increase in porewater SO_4^{2-} concentrations (Figure 6d) in the high- and low-tide seasons, respectively.

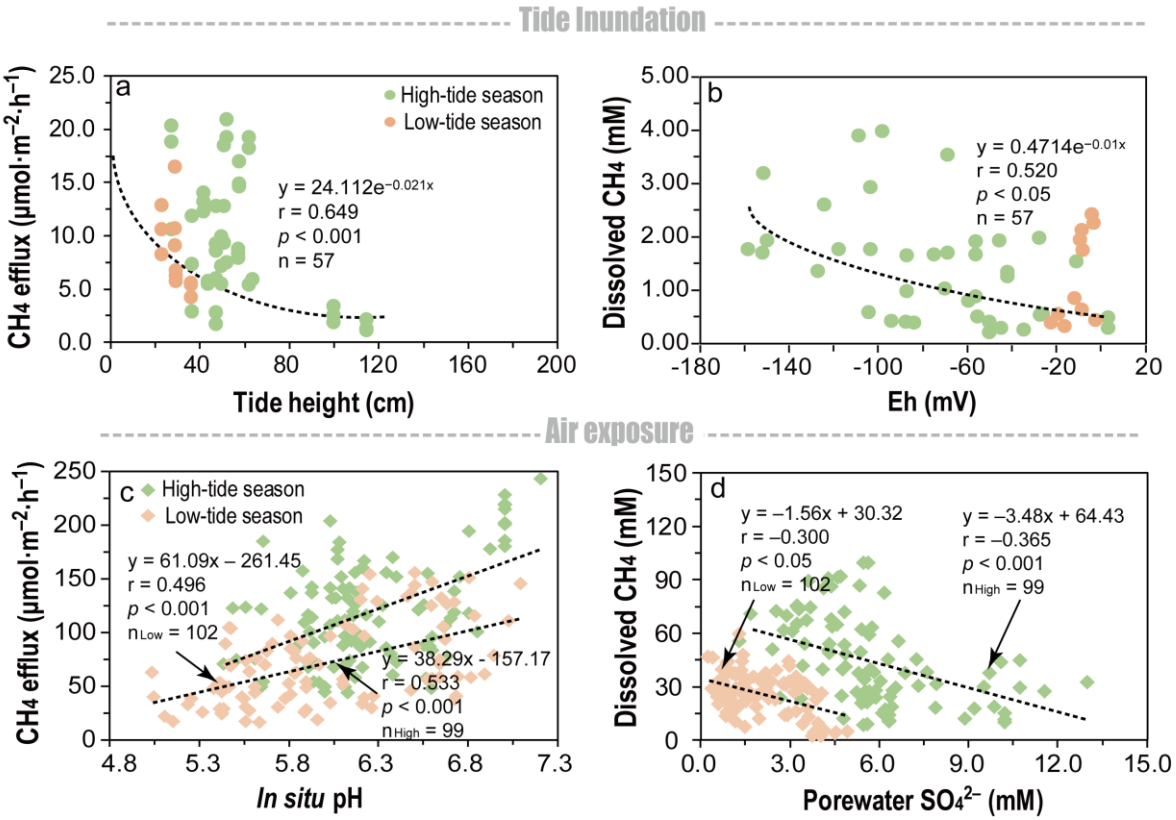

Figure 6. (**a**) Exponential regression correlation between the tide height and CH_4 effluxes; (**b**) exponential regression correlation between dissolved CH_4 concentrations and Eh, during inundation conditions; (**c**) linear regression correlation between porewater pH and CH_4 effluxes; and (**d**) linear regression correlation between dissolved CH_4 and porewater SO_4^{2-} during air-exposed conditions in high- and low-tide seasons, respectively. 'r' and 'p' refer to regression coefficient and significance level of the regression model, respectively. "n", "n_{high}", and "n_{low}" refer to the data in both high- and low-tide seasons, high-tide seasons, and low-tide seasons, respectively.

4. Discussion

The aim of this study was to explore the tidal scenario effects on CH_4 effluxes between two seasons and identify the environmental factors driving the dynamics of CH_4 effluxes during inundated and air-exposed periods in high- and low-tide seasons. Although maximal tide heights changed every day, the profiles of CH_4 effluxes and dissolved CH_4 concentrations over a tidal cycle (inundation to air-exposure to inundation) were relatively constant throughout the high-tide season (Figure 3a). By contrast, the profiles were much more heterogeneous during the low-tide season (Figure 4a), due

to the fact that the sediments were totally dried up in some periods of the tidal cycle. Our results showed that both tide inundation and seasonality showed a significant influence on CH_4 effluxes and dissolved CH_4 concentrations, and that tide inundation had a more pronounced impact on CH_4 dynamics compared with seasonal change (Figure 5).

4.1. CH_4 Effluxes and Dissolved CH_4 Concentrations during the Inundation Periods between Two Seasons

The current study identified an inverse relationship between the fluctuations in the CH_4 effluxes and the tide progression within a tidal cycle (Figures 3 and 4), and the tidewater was found to inhibit the CH_4 effluxes during each tidal cycle in both seasons (Figures 3 and 4). Then, as the sediments became exposed to air after the tidal ebb, the CH_4 effluxes rebounded to almost their original levels (Figures 3 and 4). Similar patterns have been reported in many coastal ecosystems that are frequently inundated by tidewater [7,29,30]. The cycle of inhibition and rebound occurred over a short period of time. Moreover, it was found that during periods of inundation, there was a negative exponential relationship between the magnitude of the CH_4 effluxes and the height of the tide water in both seasons (Figure 6a). A likely explanation of the inhibition is that tidewater pressure prevents diffusion of the CH_4 when the pore spaces in the sediment become filled with water [5,22,26,31,32].

The variation in the profiles of dissolved CH_4 were consistent with those of the CH_4 effluxes (Figures 3 and 4). Since the porewater sampling depth was 10–15 cm in this study, fine-grained sediments (in the form of clay and silt) likely prevented porewater exchange with the air or overlying tide water [33–36]. Dissolved CH_4 at this depth can thus be seen to a certain extent as a proxy of methanogenesis. Consistent with previous studies [29,37,38], the decreasing redox potential favored the accumulation of dissolved CH_4 during the inundation periods (Figure 6b) as the favorable redox potentials for methanogenic activity are in the range of −300 to −150 mV [10,39–41]. A reduced and anoxic environment may lead to an enrichment in methanogens, indicating that the dissolved CH_4 was indirectly affected by the redox conditions during the inundation periods.

4.2. CH_4 Effluxes and Dissolved CH_4 Concentrations during the Air-Exposed Periods between the Two Seasons

Higher CH_4 effluxes were found during the air-exposed periods in the high-tide season compared with the low-tide season (Figure 5a,b), with there being many possible explanations for this. Most importantly, the results of previous studies suggest that CH_4 effluxes are sensitive to temperature and plant growth characteristics (e.g., biomasses, primary productivities, and root exudes) [22–25], and that higher temperatures may stimulate relatively higher methanogenic activity in sediments during high-tide seasons compared with low-tide seasons [19,42,43]. In addition, as the plant biomass was more abundant in the high-tide seasons than the low-tide seasons (Table 1), this may provide more carbon-rich substrate to the methanogens [8,44].

The design of our experiment made it difficult to assess the role of the temperature, plant, or sediment and porewater geochemistries in the seasonal differences noted in the CH_4 effluxes in this study. However, we found that the porewater SO_4^{2-} and in situ pH had a definite influence on the CH_4 dynamics during the air-exposed periods within each season. During the air-exposed periods, CH_4 effluxes linearly increased with the sediment pH in the high- and low-tide seasons (Figure 6c). For each increase of one pH unit, the CH_4 effluxes significantly increased to approximately 61 and 38 mmol m^{-2} d^{-1} in the high- and low-tide seasons, respectively (Figure 6c). The most likely mechanisms by which the pH can regulate CH_4 production are related to acetoclastic methanogenesis [45]. For many mineral wetlands, the acetoclastic methanogenesis pathway has been reported to dominate CH_4 production [46], and slightly acidified sediments have been found to reduce CH_4 production in flooded rice [47], peatland [45], and tidal marsh soils [48].

Sulfates are important factors that limit methanogenesis in tidal marsh sediments [49], and the results of previous studies have found an inhibitory effect of SO_4^{2-} on the concentrations of dissolved CH_4 [50–52]. In the current study, a negative relationship was observed between the dissolved CH_4 during the air-exposed periods and the porewater SO_4^{2-} in both the high- and low-tide seasons

(Figure 6d). There are two possible explanations for this negative correlation: (i) microbial sulfate reduction is thermodynamically favored over CH_4 production in the competition for organic substrates as the metabolic process of methanogenesis yields low energy [53]; (ii) sulfate reduction is an important anaerobic CH_4 oxidation pathway in marine and coastal sediments [54,55].

4.3. Reassessment of Tide-Independent CH_4 Effluxes

In previous studies, CH_4 effluxes were typically assessed based on data from only the air-exposed periods; however, that approach may considerably overestimate the actual CH_4 efflux budget in the tidal marsh sediments. In this study, the tide height and inundation frequencies varied seasonally; however, we found that the CH_4 effluxes exponentially decreased with tide height in the inundation periods (Figure 6a). We, therefore, could estimate the seasonal CH_4 effluxes during the inundation periods using the following equation:

$$CH_4\ efflux_{inundation} = 24.112\ e^{-0.021TH}, \quad (2)$$

where $CH_4\ efflux_{inundation}$ indicates the seasonal CH_4 effluxes during the inundation periods, and TH refers to the seasonal mean tide height.

The tide height and inundation frequencies varied seasonally. With long-term observations of tide hydrological data (tide height) and using Equation (2), we could also estimate the seasonal CH_4 $efflux_{inundation}$. In addition, as shown previously [25], we had five years of observational data of seasonal CH_4 effluxes (only from air-exposure periods). Combined with this and other previous studies, we estimated the adjusted annual CH_4 effluxes (including both inundation and air-exposed periods) as follows:

$$CH_4\ efflux_{adjust} = CH_4\ efflux_{inundation} \times IR\% + CH_4\ efflux_{air\text{-}exposed} \times (1 - IR\%), \quad (3)$$

where $CH_4\ efflux_{adjust}$ refers to the adjusted annual CH_4 effluxes (containing both inundation and air-exposed periods), $CH_4\ efflux_{air\text{-}exposed}$ refers to the seasonal CH_4 effluxes during the air-exposed periods, and IR% indicates the ratio of seasonal inundation duration per month.

The results (Table 3) suggested that the adjusted seasonal CH_4 effluxes amounted to only 55–91% of the original CH_4 effluxes that were based on data obtained during the air-exposed periods. Moreover, the tide-dependent annual CH_4 efflux budget was only 76% of the original annual CH_4 efflux budget.

Table 3. Estimation of seasonal methane effluxes using tidal height and inundation frequency.

	Spring	Summer	Autumn	Winter
TH (cm)	16.4 ± 11.1	65.7 ± 13.4	123.7 ± 7.4	26.8 ± 17.7
IR (%)	13.0 ± 5.7	22.0 ± 6.8	33.6 ± 2.1	18.8 ± 7.6
$CH_4\ efflux_{air\text{-}exposed}$ ($\mu mol \cdot m^{-2} \cdot h^{-1}$)	60.8	416.3	188.6	39.5
$CH_4\ efflux_{inundation}$ ($\mu mol \cdot m^{-2} \cdot h^{-1}$)	16.4	6.1	1.8	13.7
$CH_4\ efflux_{adjust}$ ($\mu mol \cdot m^{-2} \cdot h^{-1}$)	55.0	326.0	125.8	21.9

Notes: TH refers to the seasonal mean tide height (Equation (2)); $CH_4\ efflux_{inundation}$ indicates the seasonal CH_4 effluxes during the inundation periods (Equation (2)); IR% indicates the ratios of seasonal inundation duration per month (Equation (3)); $CH_4\ efflux_{air\text{-}exposed}$ refers to the seasonal CH_4 effluxes during the inundation periods (Equation (3)); $CH_4\ efflux_{adjust}$ refers to the adjusted annual CH_4 effluxes (including both inundation and air-exposure periods; Equation (3)).

5. Conclusions

In this work, we examined the CH_4 dynamics under inundation and air-exposed periods across the high- and low-tide seasons. Our results showed that both tide inundation and seasonality showed a significant influence on CH_4 effluxes and dissolved CH_4 concentrations, and tide inundation had a more pronounced impact on CH_4 dynamics compared to seasonal change. The CH_4 effluxes during the air-exposed periods (17.6 to 248.3 $mmol \cdot m^{-2} \cdot h^{-1}$) were highly variable and generally higher than

those during inundation periods (1.0 to 22.0 mmol·m^{-2}·h^{-1}) within a tidal cycle in both seasons. Most notably, between the two seasons, the CH_4 effluxes and dissolved CH_4 concentrations from the air-exposed sediments were significantly higher during the high-tide season compared with the low-tide season, while the CH_4 effluxes and dissolved CH_4 concentrations from the inundated sediments were significantly lower during the high-tide season compared with the low-tide season. When the tide inundation frequency was taken into account, the adjusted annual budget of CH_4 effluxes amounted to 76% of the CH_4 effluxes in the air-exposed data.

To identify the effects of tidal scenarios on the CH_4 efflux dynamics in the tidal marshes, we chose the two seasons that had radically different hydrological conditions within a year. We found a significant relationship between tidal height and CH_4 efflux. However, the lack of long-term observational data limits the potential applications of this relationship. To more accurately estimate the CH_4 budget in tidal wetlands, future sampling strategies should include additional measurements of the CH_4 effluxes during both the inundation and air-exposed periods in the context of different tidal scenarios. However, tide inundation and other environmental factors, such as temperature, light, precipitation, vegetation and bioturbation, ground water table, and rise in sea-level, all vary throughout the decades, years, seasons, days, or tidal periods and, thus, intensive studies over longer time scales are needed. Even if real-time monitoring is not available, a rough first estimate of the inundated CH_4 effluxes would be possible using information on tidal heights and inundation periods.

Author Contributions: Conceptualization, M.L. and J.H.; methodology, M.L.; validation, M.L. and J.H.; investigation, M.L., J.H., Y.L., Y.Z., and J.T.; data curation, Y.L. and Y.Z.; writing—original draft preparation, M.L. and J.H.; writing—review and editing, M.L.; visualization, M.L.; supervision, M.L.; project administration, J.H.; funding acquisition, M.L. and J.H.

Funding: This research was funded by the National Science Foundation of China, grant number 41601102. This research was funded by the Key Laboratory of Wet Subtropical Ecology and Geography Process of the Ministry of Education, grant number 2017KFJJ02. This research was funded by the Key Laboratory of Coastal Environmental Processes and Ecological Remediation, YICCAS, grant number 2018KFJJ10.

Conflicts of Interest: The authors declare no conflict of interest.

References

1. IPCC. *Working Group I Contribution to the IPCC Fifth Assessment Report Climate 2013: The Physical Science Basis*; IPCC: Cambridge, UK; New York, NY, USA, 2013.
2. Borges, A.; Abril, G. *Carbon Dioxide and Methane Dynamics in Estuaries*; EGU General Assembly: Vienna, Austria, 2010; Volume 5, pp. 119–161.
3. Dame, R.; Kenny, P.D. Variability of *Spartina alterniflora* primary production in the euhaline north inlet estuary. *Mar. Ecol. Prog. Ser.* **1986**, *32*, 71–80. [CrossRef]
4. Mitsch, W.J.; Gosselink, J.G. Tidal marshes. In *Wetlands*, 5th ed.; John Wiley & Sons, Inc: Hoboken, 2015; pp. 259–310.
5. Jacotot, A.; Marchand, C.; Allenbach, M. Tidal variability of CO_2 and CH_4 emissions from the water column within a *Rhizophora mangrove* forest (New Caledonia). *Sci. Total Environ.* **2018**, *631*, 334–340. [CrossRef] [PubMed]
6. Holm, G.O.; Perez, B.C.; McWhorter, D.E.; Krauss, K.W.; Johnson, D.J.; Raynie, R.C.; Killebrew, C.J. Ecosystem level methane fluxes from tidal freshwater and brackish marshes of the Mississippi river delta: Implications for coastal wetland carbon projects. *Wetlands* **2016**, *36*, 401–413. [CrossRef]
7. Shao, X.; Sheng, X.; Wu, M.; Wu, H.; Ning, X. Methane production potential and emission at different water levels in the restored reed wetland of Hangzhou bay. *PLoS ONE* **2017**, *12*, e0185709. [CrossRef] [PubMed]
8. Yvon-Durocher, G.; Allen, A.P.; Bastviken, D.; Conrad, R.; Gudasz, C.; St-Pierre, A.; Thanh-Duc, N.; del Giorgio, P.A. Methane fluxes show consistent temperature dependence across microbial to ecosystem scales. *Nature* **2014**, *507*, 488. [CrossRef] [PubMed]
9. Luo, M.; Huang, J.; Zhu, W.; Tong, C. Impacts of increasing salinity and inundation on rates and pathways of organic carbon mineralization in tidal wetlands: A review. *Hydrobiologia* **2019**, *827*, 31–49. [CrossRef]

10. Taillefert, M.; Neuhuber, S.; Bristow, G. The effect of tidal forcing on biogeochemical processes in intertidal salt marsh sediments. *Geochem. Trans.* **2007**, *8*, 1–15. [CrossRef]
11. Chen, X.; Slater, L. Methane emission through ebullition from an estuarine mudflat: I. A conceptual model to explain tidal forcing based on effective stress changes. *Water Resour. Res.* **2016**, *52*, 4469–4485. [CrossRef]
12. Li, X.; Mitsch, W.J. Methane emissions from created and restored freshwater and brackish marshes in southwest Florida, USA. *Ecol. Eng.* **2016**, *91*, 529–536. [CrossRef]
13. McClain, M.E.; Boyer, E.W.; Dent, C.L.; Gergel, S.E.; Grimm, N.B.; Groffman, P.M.; Hart, S.C.; Harvey, J.W.; Johnston, C.A.; Mayorga, E.; et al. Biogeochemical hot spots and hot moments at the interface of terrestrial and aquatic ecosystems. *Ecosystems* **2003**, *6*, 301–312. [CrossRef]
14. Sturm, K.; Werner, U.; Grinham, A.; Yuan, Z. Tidal variability in methane and nitrous oxide emissions along a subtropical estuarine gradient. *Estuar. Coast. Shelf Sci.* **2017**, *192*, 159–169. [CrossRef]
15. Welti, N.; Hayes, M.; Lockington, D. Seasonal nitrous oxide and methane emissions across a subtropical estuarine salinity gradient. *Biogeochemistry* **2017**, *132*, 55–69. [CrossRef]
16. Zhang, Y.; Ding, W. Diel methane emissions in stands of *Spartina alterniflora* and *Suaeda salsa* from a coastal salt marsh. *Aquat. Bot.* **2011**, *95*, 262–267. [CrossRef]
17. Hirota, M.; Senga, Y.; Seike, Y.; Nohara, S.; Kunii, H. Fluxes of carbon dioxide, methane and nitrous oxide in two contrastive fringing zones of coastal lagoon, lake Nakaumi, Japan. *Chemosphere* **2007**, *68*, 597–603. [CrossRef] [PubMed]
18. Rosentreter, J.A.; Maher, D.T.; Erler, D.V.; Murray, R.H.; Eyre, B.D. Methane emissions partially offset 'blue carbon' burial in mangroves. *Sci. Adv.* **2018**, *4*. [CrossRef]
19. Li, H.; Dai, S.; Ouyang, Z.; Xie, X.; Guo, H.; Gu, C.; Xiao, X.; Ge, Z.; Peng, C.; Zhao, B. Multi-scale temporal variation of methane flux and its controls in a subtropical tidal salt marsh in eastern China. *Biogeochemistry* **2018**, *137*, 163–179. [CrossRef]
20. Sun, Z.; Sun, W.; Tong, C.; Zeng, C.; Yu, X.; Mou, X. China's coastal wetlands: Conservation history, implementation efforts, existing issues and strategies for future improvement. *Environ. Int.* **2015**, *79*, 25–41. [CrossRef]
21. Menéndez, M.; Woodworth, P.L. Changes in extreme high water levels based on a quasi-global tide-gauge data set. *J. Geophys. Res. Ocean.* **2010**, *115*. [CrossRef]
22. Tong, C.; Huang, J.F.; Hu, Z.Q.; Jin, Y.F. Diurnal variations of carbon dioxide, methane, and nitrous oxide vertical fluxes in a subtropical estuarine marsh on neap and spring tide days. *Estuar. Coasts* **2013**, *36*, 633–642. [CrossRef]
23. Hu, M.; Wilson, B.J.; Sun, Z.; Ren, P.; Tong, C. Effects of the addition of nitrogen and sulfate on CH_4 and CO_2 emissions, soil, and pore water chemistry in a high marsh of the Min river estuary in southeastern China. *Sci. Total Environ.* **2017**, *579*, 292–304. [CrossRef]
24. Tong, C.; Wang, W.; Huang, J.; Gauci, V.; Zhang, L.; Zeng, C. Invasive alien plants increase CH_4 emissions from a subtropical tidal estuarine wetland. *Biogeochemistry* **2012**, *111*, 677–693. [CrossRef]
25. Yang, P.; Wang, M.; Lai, D.Y.; Chun, K.; Huang, J.; Wan, S.; Bastviken, D.; Tong, C. Methane dynamics in an estuarine brackish *Cyperus malaccensis* marsh: Production and porewater concentration in soils, and net emissions to the atmosphere over five years. *Geoderma* **2019**, *337*, 132–142. [CrossRef]
26. Tong, C.; Wang, W.; Zeng, C.; Marrs, R. Methane (CH_4) emission from a tidal marsh in the Min river estuary, southeast China. *J. Environ. Sci. Heal. A* **2010**, *45*, 506–516. [CrossRef]
27. Xiao, L.; Xie, B.; Liu, J.; Zhang, H.; Han, G.; Wang, O.; Liu, F. Stimulation of long-term ammonium nitrogen deposition on methanogenesis by *Methanocellaceae* in a coastal wetland. *Sci. Total Environ.* **2017**, *595*, 337–343. [CrossRef] [PubMed]
28. Keller, J.K.; Weisenhorn, P.B.; Megonigal, J.P. Humic acids as electron acceptors in wetland decomposition. *Soil Biol. Biochem.* **2009**, *41*, 1518–1522. [CrossRef]
29. Barnes, J.; Ramesh, R.; Purvaja, R.; Nirmal Rajkumar, A.; Senthil Kumar, B.; Krithika, K.; Ravichandran, K.; Uher, G.; Upstill-Goddard, R. Tidal dynamics and rainfall control N_2O and CH_4 emissions from a pristine mangrove creek. *Geophys. Res. Lett.* **2006**, *33*. [CrossRef]
30. Kroeger, K.D.; Crooks, S.; Moseman-Valtierra, S.; Tang, J. Restoring tides to reduce methane emissions in impounded wetlands: A new and potent blue carbon climate change intervention. *Sci. Rep.* **2017**, *7*, 11914. [CrossRef] [PubMed]

31. Yamamoto, A.; Hirota, M.; Suzuki, S.; Oe, Y.; Zhang, P.; Mariko, S. Effects of tidal fluctuations on CO_2 and CH_4 fluxes in the littoral zone of a brackish-water lake. *Limnology* **2009**, *10*, 229–237. [CrossRef]
32. Yamamoto, A.; Hirota, M.; Suzuki, S.; Zhang, P.; Mariko, S. Surrounding pressure controlled by water table alters CO_2 and CH_4 fluxes in the littoral zone of a brackish-water lake. *Appl. Soil Ecol.* **2011**, *47*, 160–166. [CrossRef]
33. Bahlmann, E.; Weinberg, I.; Lavrič, J.; Eckhardt, T.; Michaelis, W.; Santos, R.; Seifert, R. Tidal controls on trace gas dynamics in a seagrass meadow of the Ria Formosa lagoon (southern Portugal). *Biogeosciences* **2015**, *12*, 1683–1696. [CrossRef]
34. Kostka, J.E.; Gribsholt, B.; Petrie, E.; Dalton, D.; Skelton, H.; Kristensen, E. The rates and pathways of carbon oxidation in bioturbated saltmarsh sediments. *Limnol. Oceanogr.* **2002**, *47*, 230–240. [CrossRef]
35. Nóbrega, G.; Ferreira, T.; Romero, R.; Marques, A.; Otero, X. Iron and sulfur geochemistry in semi-arid mangrove soils (Ceará, Brazil) in relation to seasonal changes and shrimp farming effluents. *Environ. Monit. Assess.* **2013**, *185*, 7393–7407. [CrossRef] [PubMed]
36. Segarra, K.; Schubotz, F.; Samarkin, V.; Yoshinaga, M.; Hinrichs, K.; Joye, S. High rates of anaerobic methane oxidation in freshwater wetlands reduce potential atmospheric methane emissions. *Nat. Commun.* **2015**, *6*, 7477. [CrossRef] [PubMed]
37. De La Paz, M.; Gómez-Parra, A.; Forja, J. Tidal-to-seasonal variability in the parameters of the carbonate system in a shallow tidal creek influenced by anthropogenic inputs, Rio San Pedro (SW Iberian peninsula). *Cont. Shelf Res.* **2008**, *28*, 1394–1404. [CrossRef]
38. Deborde, J.; Anschutz, P.; Guérin, F.; Poirier, D.; Marty, D.; Boucher, G.; Thouzeau, G.; Canton, M.; Abril, G. Methane sources, sinks and fluxes in a temperate tidal lagoon: The Arcachon lagoon (SW France). *Estuar. Coast. Shelf Sci.* **2010**, *89*, 256–266. [CrossRef]
39. Koh, H.-S.; Ochs, C.A.; Yu, K. Hydrologic gradient and vegetation controls on CH_4 and CO_2 fluxes in a spring-fed forested wetland. *Hydrobiologia* **2009**, *630*, 271–286. [CrossRef]
40. Passeri, D.L.; Hagen, S.C.; Medeiros, S.C.; Bilskie, M.V.; Alizad, K.; Wang, D. The dynamic effects of sea level rise on low-gradient coastal landscapes: A review. *Earth's Future* **2015**, *3*, 159–181. [CrossRef]
41. Yu, K.; Faulkner, S.P.; Patrick, W.H., Jr. Redox potential characterization and soil greenhouse gas concentration across a hydrological gradient in a Gulf coast forest. *Chemosphere* **2006**, *62*, 905–914. [CrossRef]
42. Inglett, P.; Inglett, K. Biogeochemical changes during early development of restored calcareous wetland soils. *Geoderma* **2013**, *192*, 132–141. [CrossRef]
43. Parashar, D.; Gupta, P.K.; Rai, J.; Sharma, R.; Singh, N. Effect of soil temperature on methane emission from paddy fields. *Chemosphere* **1993**, *26*, 247–250. [CrossRef]
44. Schütz, H.; Seiler, W.; Conrad, R. Influence of soil temperature on methane emission from rice paddy fields. *Biogeochemistry* **1990**, *11*, 77–95. [CrossRef]
45. Ye, R.; Doane, T.A.; Morris, J.; Horwath, W.R. The effect of rice straw on the priming of soil organic matter and methane production in peat soils. *Soil Biol. Biochem.* **2015**, *81*, 98–107. [CrossRef]
46. Dettling, M.D.; Yavitt, J.B.; Cadillo-Quiroz, H.; Sun, C.; Zinder, S.H. Soil-methanogen interactions in two peatlands (bog, fen) in central New York state. *Geomicrobiol. J.* **2007**, *24*, 247–259. [CrossRef]
47. Wang, Z.; Delaune, R.; Patrick, W.; Masscheleyn, P. Soil redox and pH effects on methane production in a flooded rice soil. *Soil Sci. Soc. Am. J.* **1993**, *57*, 382–385. [CrossRef]
48. Keller, J.K.; Bridgham, S.D. Pathways of anaerobic carbon cycling across an ombrotrophic-minerotrophic peatland gradient. *Limnol. Oceanogr.* **2007**, *52*, 96–107. [CrossRef]
49. Herbert, E.R.; Boon, P.; Burgin, A.J.; Neubauer, S.C.; Franklin, R.B.; Ardón, M.; Hopfensperger, K.N.; Lamers, L.P.; Gell, P. A global perspective on wetland salinization: Ecological consequences of a growing threat to freshwater wetlands. *Ecosphere* **2015**, *6*, 1–43. [CrossRef]
50. Bartlett, K.B.; Bartlett, D.S.; Harriss, R.C.; Sebacher, D.I. Methane emissions along a salt marsh salinity gradient. *Biogeochemistry* **1987**, *4*, 183–202. [CrossRef]
51. Chambers, L.G.; Reddy, K.R.; Osborne, T.Z. Short-term response of carbon cycling to salinity pulses in a freshwater wetland. *Soil Sci. Soc. Am. J.* **2011**, *75*, 2000–2007. [CrossRef]
52. Weston, N.B.; Dixon, R.E.; Joye, S.B. Ramifications of increased salinity in tidal freshwater sediments: Geochemistry and microbial pathways of organic matter mineralization. *J. Geophys. Res. Biogeosci.* **2006**, *111*, 1–14. [CrossRef]

53. Stumm, W.; Morgan, J.J. *Aquatic Chemistry: Chemical Equilibria and Rates in Natural Waters*; Wiley: New York, NY, USA, 1996.
54. Boetius, A.; Ravenschlag, K.; Schubert, C.J.; Rickert, D.; Widdel, F.; Gieseke, A.; Amann, R.; Jørgensen, B.B.; Witte, U.; Pfannkuche, O. A marine microbial consortium apparently mediating anaerobic oxidation of methane. *Nature* **2000**, *407*, 623. [CrossRef]
55. RoyChowdhury, T.; Bramer, L.; Hoyt, D.W.; Kim, Y.-M.; Metz, T.O.; McCue, L.A.; Diefenderfer, H.L.; Jansson, J.K.; Bailey, V. Temporal dynamics of CO_2 and CH_4 loss potentials in response to rapid hydrological shifts in tidal freshwater wetland soils. *Ecol. Eng.* **2018**, *114*, 104–114. [CrossRef]